1521-0103/365/2/262–271$35.00
THE JOURNAL OF PHARMACOLOGY AND EXPERIMENTAL THERAPEUTICS

https://doi.org/10.1124/jpet.117.247296
J Pharmacol Exp Ther 365:262–271, May 2018

Establishing Transcriptional Signatures to Differentiate PXR-, CAR-, and AhR-Mediated Regulation of Drug Metabolism and Transport Genes in Cryopreserved Human Hepatocytes

Jamie E. Moscovitz, Amit S. Kalgutkar, Kelly Nulick, Nathaniel Johnson, Zhiwu Lin, Theunis C. Goosen, and Yan Weng

Medicine Design, Pfizer Inc., Cambridge, Massachusetts (J.E.M., A.S.K., Y.W.), and Medicine Design, Pfizer Inc., Groton, Connecticut (K.N., N.J., Z.L., T.C.G.)

Received December 18, 2017; accepted February 8, 2018

ABSTRACT

The potential for drug-drug interactions (DDIs) arising from transcriptional regulation of drug-disposition genes via activation of nuclear receptors (NRs), such as pregnane X receptor (PXR), constitutive androstane receptor (CAR), and aryl hydrocarbon receptor (AhR), remains largely unexplored, as highlighted in a recent guidance document from the European Medicines Agency. The goal of this research was to establish PXR-/CAR-/AhR-specific drug-metabolizing enzyme (DME) and transporter gene expression signatures in sandwich-cultured cryopreserved human hepatocytes using selective activators of PXR (rifampin), CAR (CITCO), and AhR (omeprazole). Dose response for ligand-induced changes to 38 major human DMEs and critical hepatobiliary transporters were assessed using a custom gene expression array card. We identified novel differentially expressed drug-disposition genes for PXR (↑ABCB1/MDR1, CYP2C9, CYP2C19, and EPHX1, ↓ABCB11), CAR [↑sulfotransferase (SULT) 1E1, uridine glucuronosyl transferase (UGT) 2B4], and AhR (↑SLC10A1/NTCP, SLCO1B1/OATP1B1], and coregulated genes (CYP1A1, CYP2B6, CYP2C8, CYP3A4, UGT1A1, UGT1A4). Subsequently, DME gene expression signatures were generated for known CYP3A4 inducers PF-06282999 and pazopanib. The former produced an induction signature almost identical to that of rifampin, suggesting activation of the PXR pathway, whereas the latter produced an expression signature distinct from those of PXR, CAR, or AhR, suggesting involvement of an alternate pathway(s). These results demonstrate that involvement of PXR/CAR/AhR can be identified via expression changes of signature DME/transporter genes. Inclusion of such signature genes could serve to simultaneously identify potential inducers and inhibitors, and the NRs involved in the transcriptional regulation, thus providing a more holistic and mechanism-based assessment of DDI risk for DMEs and transporters beyond conventional cytochrome P450 isoforms.

Introduction

Examination of the potential for clinical drug-drug interactions (DDIs) with investigational drugs is examined through in vitro inhibition of the catalytic activities of hepatic phase I and phase II drug-metabolizing enzymes (DMEs) [e.g., cytochrome P450 (P450) and uridine glucuronosyl transferases (UGTs)] (Williams et al., 2004; Wienkers and Heath, 2005; Chu et al., 2009; NDA-022465, 2009) and hepatobiliary transporter-mediated uptake [e.g., organic anion-transporting polypeptide (solute carrier *SLCO*/OATP isoforms)] and efflux [e.g., multidrug resistant gene [ATP-binding cassette (*ABCB*/MDR)1 and breast cancer resistance protein (*ABCG2*/BCRP)] (Giacomini et al., 2010). An additional source of DDIs can involve regulation of drug-disposition genes through activation of nuclear receptors (NRs), including pregnane X receptor (PXR), constitutive androstane receptor (CAR), and/or aryl hydrocarbon receptor (AhR) (Goodwin et al., 2002a; Willson and Kliewer, 2002; Xu et al., 2005). Quantitative assessment of DDI risk via NR activation uses primary human hepatocytes and focuses almost exclusively on the messenger RNA (*m*RNA) and catalytic activity increases in the major constitutively expressed human P450 isoform CYP3A4 (along with CYP2B6 and CYP1A1/2). Whereas prominent induction of CYP1A1/2 is a hallmark feature of AhR activation (Fahmi and Ripp, 2010), induction of human CYP3A4 or CYP2B6 can be coregulated by PXR and CAR (Lehmann et al., 1998; Goodwin et al., 1999, 2002a,b).

This work was supported by a Pfizer Worldwide Research and Development Postdoctoral Fellowship Award to J.E.M.
https://doi.org/10.1124/jpet.117.247296.

ABBREVIATIONS: ABC, ATP-binding cassette; AhR, aryl hydrocarbon receptor; ANOVA, analysis of variance; AUC, area under the plasma concentration time curve; BCRP, breast cancer resistance protein; CAR, constitutive androstane receptor; cDNA, complementary DNA; CES, carboxylesterase; CITCO, 6-(4-chlorophenyl)imidazo[2,1-*b*][1,3]thiazole-5-carbaldehyde *O*-(3,4-dichlorobenzyl)oxime; C_{max}, maximal plasma concentration; DDI, drug-drug interaction; DME, drug-metabolizing enzyme; DMSO, dimethylsulfoxide; E_{max}, maximum effect; EPHX, epoxide hydrolase; GST, glutathione-*S*-transferase; HSD, hydroxysteroid dehydrogenase; MDR, multidrug resistant protein; MOI, maximal observed induction; *m*RNA, messenger RNA; MRP, multidrug resistance–associated protein; NR, nuclear receptor; OATP, organic anion-transporting polypeptide; OCT, organic cation transporter; PF-06282999, 2-(6-(5-chloro-2-methoxyphenyl)-4-oxo-2-thioxo-3,4-dihydropyrimidin-1(2*H*)-yl)-acetamide; PPARα, peroxisome proliferator-activated receptor α; PXR, pregnane X receptor; qPCR, quantitative polymerase chain reaction; SLC, solute carrier transporter; SULT, sulfotransferase; TKI, tyrosine kinase inhibitor; UGT, uridine glucuronosyl transferase.

NR-mediated transcriptional regulation pathways are associated with characteristic and oftentimes overlapping target drug-disposition genes (Willson and Kliewer, 2002; Xu et al., 2005; Aleksunes and Klaassen, 2012; Wang et al., 2012); however, little is known regarding the potential of xenobiotics (including drugs) to regulate DMEs other than CYP1A2/2B6/3A4, a deficiency that is specifically noted in the European Medicines Agency (EMA) Guidelines on the investigation of drug interaction document (EMA, 2012). These deficiencies have also been highlighted by the Induction Working Group of the Innovation and Quality Consortium with regard to gaining a fundamental understanding of the mechanism(s) and implications of downregulation of drug-disposition genes (Hariparsad et al., 2017). A recent examination, which correlated physiochemical properties of ~300 compounds with respect to induction of P450 and transporter *m*RNA in human hepatocytes, demonstrated that induction of CYP1A2/2B6/3A4 *m*RNAs was observed with 16%–33% of the test compounds (Badolo et al., 2015). In contrast, transporter *m*RNAs [e.g., OATP1B1, organic cation transporter *SLC22A1*/OCT1, MDR1, multidrug resistance associated proteins *ABCC*/MRP2 and 3 and BCRP] were induced by <10% of the tested compounds. Many of the active compounds, however, induced multiple DMEs and/or transporters (Badolo et al., 2015). Kandel et al. (2016) also assessed genome-wide changes to transcriptional pathways on the induction of PXR, CAR, and peroxisome proliferator-activated receptor α (PPARα) after treatment of human hepatocytes with rifampin (PXR activator), 6-(4-chlorophenyl)imidazo[2,1-*b*][1,3]thiazole-5-carbaldehyde O-(3,4-dichlorobenzyl)oxime (CITCO, CAR activator), or WY14,643 (PPARα activator). Although not specifically focused on DME and xenobiotic transport networks, this work confirmed several drug-disposition genes that were among the top 25 upregulated *m*RNAs for each pathway, including CYP2B6/2C8/2C9/3A4 (PXR), CYP1A1/2/2B6/2C8/2C9/3A4 (CAR), and CYP2C8/3A4 (PPARα) (Kandel et al., 2016). These observations represent a pragmatic first step in the holistic analysis of genes subject to NR-mediated transcriptional regulation; however, the analysis is limited to the use of a single NR activator concentration in assessment of transcriptional regulation of major DMEs and transporters.

The present account summarizes our work on the categorization of multiple signature genes (Table 1) in human hepatocytes, which can mediate the metabolism or hepatobiliary disposition of xenobiotics and small-molecule drugs, as qualitative biomarkers for activation of PXR, CAR, or AhR by prototypic and selective activators rifampin, CITCO, and omeprazole, respectively (Fig. 1). Concentration-response relationships were explored to allow for the determination of EC_{50} and maximum effect (E_{max}) values to aid in the interpretation of individual *m*RNA induction data. The ability of genes to serve as qualitative biomarkers for specific PXR, CAR, or AhR activation was further tested with two structurally diverse compounds, namely, 2-(6-(5-chloro-2-methoxyphenyl)-4-oxo-2-thioxo-3,4-dihydropyrimidin-1(2*H*)-yl)-acetamide (PF-06282999) and pazopanib (Fig. 1). PF-06282999 is a thiouracil-based irreversible inhibitor of the myeloperoxidase enzyme (Ruggeri et al., 2015; Dong et al., 2016), which induces CYP3A4 *m*RNA and catalytic activity via PXR (but not CAR1 or CAR3) transactivation (Moscovitz et al., 2017) and causes statistically significant decreases in the systemic exposure of CYP3A4 substrate midazolam in healthy adult subjects (Dong et al., 2017). Pazopanib, an indazolylpyrimidine-based tyrosine kinase inhibitor (TKI), is a substrate (Keisner and Shah, 2011; Liu et al., 2016) and inhibitor (Hamberg et al., 2015) of CYP3A4. In vitro studies in human hepatocytes suggest pazopanib to be a moderate inducer of CYP3A4 and CYP2B6 *m*RNA and catalytic activities, presumably via PXR activation (https://www.accessdata.fda.gov/drugsatfda_docs/nda/2009/022465s000_ClinPharmR.pdf).

Materials and Methods

Materials. PF-06282999 (chemical purity >99% by high-performance liquid chromatography and nuclear magnetic resonance) was synthesized at Pfizer Worldwide Research and Development (Groton, CT). Hepatocyte thawing, plating, and incubation medium, as well as the Torpedo antibiotic mix for the medium, were purchased from Bioreclamation IVT Celsis (Baltimore, MD) and CellzDirect (Pittsboro, NC). Rifampin, CITCO, omeprazole, pazopanib, Dulbecco's phosphate-buffered saline, and dimethylsulfoxide (DMSO) were purchased from Sigma-Aldrich (St. Louis, MO). Cryopreserved human hepatocyte lots were purchased as follows: HH1089 (white woman, aged 57 years), In Vitro ADMET Laboratories (Columbia, MD); FOS (Arabic man, aged 34 years), and BNA (white man, aged 43 years) Bioreclamation IVT Celsis.

NR Transactivation Assays. Human PXR transactivation was determined by luciferase activity using a proprietary reporter cell-based assay according to the manufacturer's protocol (Indigo Biosciences, State College, PA). The assay uses reporter cells expressing a hybrid form of PXR containing native human PXR-ligand binding domain and the yeast GAL4-DNA binding domain, which regulates

TABLE 1
List of signature drug metabolizing enzyme and transporter genes included in panel

Phase I	Phase II	Uptake Transporters	Efflux Transporters	NRs + Non-DME Targets
AOX1	GSTA1	SLC10A1/NTCP	ABCB1/MDR1	AhR
CES1	GSTP1	SLC22A1/OCT1	ABCB4/MDR3	NR0B2/SHP
CYP1A1	SULT1E1	SLC22A7/OAT2	ABCB11/BSEP	NR1H4/FXR
CYP2B6	UGT1A1	SLC47A1/MATE1	ABCC2/MRP2	NR1I2/PXR
CYP2C8	UGT1A4	SLCO1B1/OATP1B1	ABCC3/MRP3	NR1I3/CAR
CYP2C9	UGT1A6	SLCO1B3/OATP1B3	ABCC4/MRP4	PDK4
CYP2C19	UGT1A9	SLCO2B1/OATP2B1	ABCC5/MRP5	PPARα
CYP2D6	UGT2B4		ABCC6/MRP6	
CYP3A4	UGT2B7		ABCG2/BCRP	
EPHX1	UGT2B15			
EPHX2				
HSD11β1				

AOX, aldehyde oxidase; BSEP, bile salt export salt; CES1, carboxylesterase 1; FXR, farnesoid X receptor; OCT1 organic cation transporter 1; PDK4, pyruvate dehydrogenase kinase 4; SHP, small heterodimer partner (also known as NR0B2).

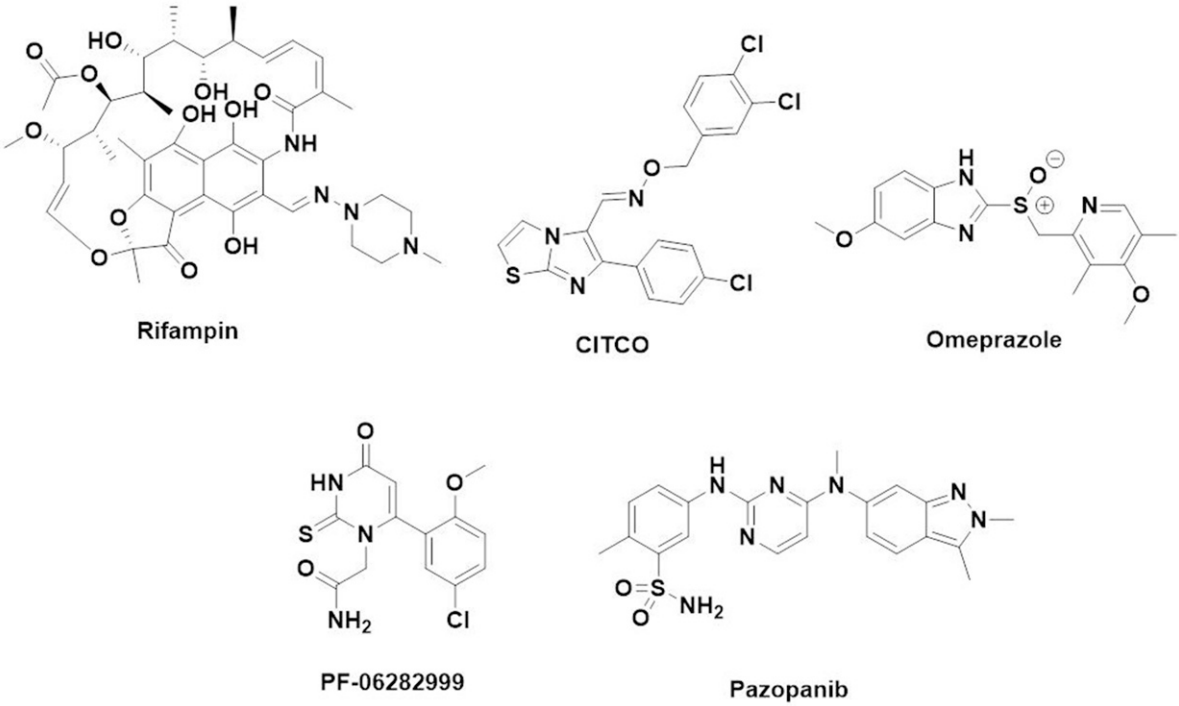

Fig. 1. Chemical structures of the PXR agonists rifampin and PF-06282999, CAR agonist CITCO, AhR agonist omeprazole, and tyrosine kinase inhibitor pazopanib.

the expression of a luciferase reporter gene. Human CAR1 and CAR3 transactivation assays were conducted according to the manufacturer's recommendations (Puracyp, Inc., Carlsbad, CA). The assay consists of hepatoma cells transiently transfected with the full-length human CAR, splice variant 1 or 3, and a luciferase reporter gene linked to the human promoters XRE and PXRE. Human AhR transactivation assays were conducted by Puracyp, Inc. This assay uses stably transfected proprietary reporter cells with the full-length human AhR and a luciferase reporter gene linked to the human CYP1A2 promoter dioxin response elements. For all transactivation assays, reporter cells were seeded into a 96-well format assay plate and preincubated from 4 to 12 hours. Treatment followed with medium containing solvent (0.1% DMSO) control, rifampin (0.03–30 μM), CITCO (0.005–20 μM), or omeprazole (0.3–300 μM), after which medium was discarded and luciferase detection reagent was added to detect luciferase activity. The intensity of light emission from each assay well was quantified using a plate-reading luminometer.

Human Hepatocyte Culture and Treatment. Cryopreserved human hepatocytes (three donors per experiment) were used to examine *m*RNA using established protocols (Fahmi et al., 2008b). The plates were overlaid with 0.25 mg/ml Matrigel 4 hours after plating, and the cultures were maintained in InVitroGro-HI medium. Hepatocytes were seeded in collagen I-precoated 48-well plates, and each well had a cell density of ~1.6×10^5 viable cells. One day after plating, hepatocyte cultures were treated for 48 hours with medium containing solvent control (0.1% DMSO), rifampin (0.1–10 μM), CITCO (0.001–1 μM), omeprazole (0.03–3 μM), PF-06282999 (10–1000 μM), or pazopanib (0.1–10 μM) in triplicate. Final concentrations of rifampin, CITCO, and omeprazole were chosen based on selectivity of specific activators in NR transactivation assays.

RNA Isolation and Gene Expression Assays. Cryopreserved human hepatocytes were washed with phosphate-buffered saline, and total RNA was isolated using an RNeasy Kit (Qiagen, Valencia, CA) according to the manufacturer's recommendations. RNeasy lysis buffer (Buffer RLT) with 1% β-mercaptoethanol was applied to plates and placed on a plate shaker for 10 minutes at 800 rpm. The concentration and purity of RNA were assessed using the Nanodrop 8000 spectrophotometer (Thermo Scientific, Wilmington, DE). Complementary DNA (cDNA) was generated using High-Capacity cDNA Synthesis (Applied Biosystems, Foster City, CA). *m*RNA expression was determined by quantitative polymerase chain reaction (qPCR) using a custom TaqMan array card containing 35 representative hepatic phase I and II DMEs [P450s, UGTs, sulfotransferases (SULTs), glutathione-*S*-transferases (GSTs), aldehyde oxidase, carboxylesterase (CES), epoxide hydrolase (EPHX)], hydroxysteroid dehydrogenase (HSD)11β1, and hepatobiliary transporters (SLC, SLCO, ABC) (Table 1). In addition to hepatic DMEs and transporters, non-drug disposition genes, typically used as indicators for NR activation were also included as controls (NRs and Non-DME targets, Table 1). Approximately 50 ng of cDNA per sample was loaded per port. Array cards were briefly centrifuged and sealed, and qPCR was performed with a ViiA7 Real-Time PCR machine (Life Technologies, Grand Island, NY). Gene expression was analyzed using Expression Suite (Life Technologies) software. The relative quantity of each target gene compared with an endogenous control gene (glyceraldehyde-3-phosphate dehydrogenase) was calculated using the $\Delta\Delta$CT method.

Data Analysis. Transactivation assay data from reporter cell lines are presented as mean ± S.D. *m*RNA expression data from cryopreserved human hepatocyte experiments are presented as mean ± S.E. Statistical analysis was performed using GraphPad Prism v7 (La Jolla, CA). *m*RNA expression data were plotted versus the concentration of rifampin, CITCO, omeprazole, PF-06282999, or pazopanib. Individual fitting was carried out on each hepatocyte donor using GraphPad Prism version 7 and was fit to either a four-parameter sigmoidal model (fitting E_{max}, Hill slope, and EC_{50}, with baseline fixed at 1) or three-parameter sigmoidal model (fitting E_{max} and EC_{50}, with Hill slope and baseline each fixed at 1). The four-parameter model was preferred if adding the extra parameter produced a fit with $P < 0.05$ compared with the three-parameter model by the built-in GraphPad extra sum-of-squares F test. mRNA expression was analyzed by a two-way ANOVA followed by a Dunnett's multiple comparison test to compare overall mean differences between treatment groups. Significance was set at $P < 0.05$.

Results

PXR-, CAR-, and AhR-Specific Induction Signatures Based on Maximal Observed Induction. For each agonist, a minimum of five concentrations in the range of 0.1–10 μM for rifampin, 0.01–1 μM for CITCO, and 0.03–3 μM for omeprazole were selected based on the specificity of each compound for its respective NR, as determined in the transactivation assays (Fig. 2). *m*RNA expression was analyzed by qPCR with TaqMan array cards, normalized to vehicle control, and relative fold induction was plotted versus the concentration dose response for each agonist and donor hepatocyte lot. A maximal observed induction (MOI) was reported for each gene in each of the individual donor lots, and these data were averaged and visualized by heat maps (Fig. 3), with average relative fold induction/MOI indicated next to each gene name. After treatment of human hepatocytes (BNA, FOS, and HH1089 lots) with NR agonists, intervariability in fold induction of *m*RNA of several genes was observed among the individual lots, as noted in previous studies (Fahmi et al., 2008a,b). In general, BNA was the most sensitive to *m*RNA induction by PXR, CAR, and AhR activators, followed by FOS and HH1089. Despite the variability in magnitude, the patterns of target gene induction, the relative sensitivity of target genes (compared among each other for a particular donor lot), and the minimal day-to-day experimental variation remained consistent.

Activation of PXR, CAR, and AhR by selective activators rifampin, CITCO, and omeprazole, respectively, resulted in differing gene expression profiles and magnitude of induction for target genes (Fig. 3A). Rifampin, CITCO, and omeprazole treatment led to selective induction of CYP3A4, CYP2B6, and CYP1A1 mRNA by 75-fold, 22-fold, and 37-fold, respectively, in the three human-hepatocyte donor lots. In addition, rifampin treatment induced CYP2B6 and CYP2C8 >10-fold, as well as UGT1A4, UGT1A1, CYP2C19, and CYP2C9 between 3- and 5-fold. Likewise, CAR activation by CITCO induced phase I and II DMEs and transporters, albeit in a less robust fashion than rifampin, including CYP3A4, CYP2C8, UGT1A1, SULT1E1, and UGT1A4 between 2- and 5-fold. Subsequent to CYP1A1, omeprazole most prominently induced CYP2B6 (14-fold↑) and UGT1A1, SLC10A1, SLCO1B1, and CYP3A4 (2- to 3-fold↑). qPCR quantification of *m*RNA expression was also able to detect the downregulation of genes included in the panel, which was a considerably less frequent event than upregulation. Rifampin treatment resulted in significant downregulation of ABCB11 (Fig. 3). No significant downregulation of DMEs or transporters included in the panel was observed with CITCO or omeprazole activation of CAR and AhR, respectively.

Lot-to-lot variability of cryopreserved human hepatocytes has been described in the literature via ranges of CYP3A4 EC_{50} and E_{max} values (Fahmi et al., 2008a,b), as well as principal component analysis (Kandel et al., 2016) of multiple donors. As such, this variability was considered in our assessment of true signature genes, and only those that were robustly reproducible across donors were included as a final signature gene in response to a PXR, CAR, or AhR activator (Fig. 4). Criteria as a signature gene (upregulation or downregulation) for an NR included statistically significant induction (≥2-fold) relative to vehicle control, as determined by two-way ANOVA followed by a Dunnett's multiple comparison test in two or more donors and at one or more concentrations. PXR-specific target genes included ABCB1, CYP2C9, CYP2C19, and EPHX1. CAR-specific target genes included SULT1E1 and UGT2B4, whereas AhR alone significantly induced SLC10A1 and SLCO1B1. PXR and CAR coregulated CYP2B6, CYP2C8, and UGT1A4, whereas CYP1A1, CYP3A4, and UGT1A1 were upregulated upon activation of all three NRs.

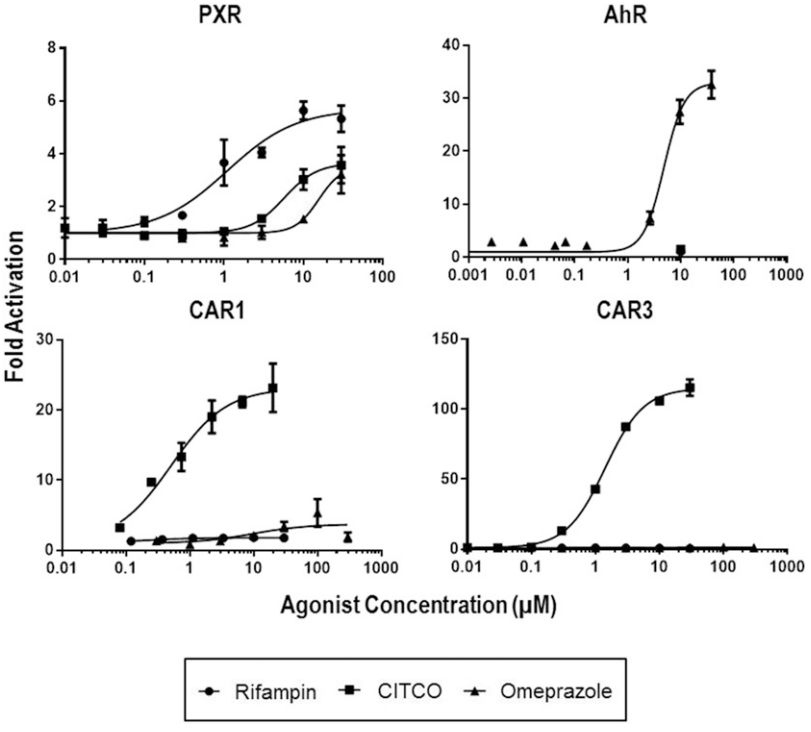

Fig. 2. Selection of activator concentration range with PXR, CAR, and AhR transactivation in luciferase-based reporter assay. Reporter cells were treated with solvent (0.1% DMSO) control, rifampin (0.03–30 μM), CITCO (0.005–20 μM), or omeprazole (0.3–300 μM), after which the drug-containing medium was removed and replaced with medium containing luciferase detection reagent, and luminescence was measured on a luminometer. All sigmoidal dose-response data were fit by nonlinear regression.

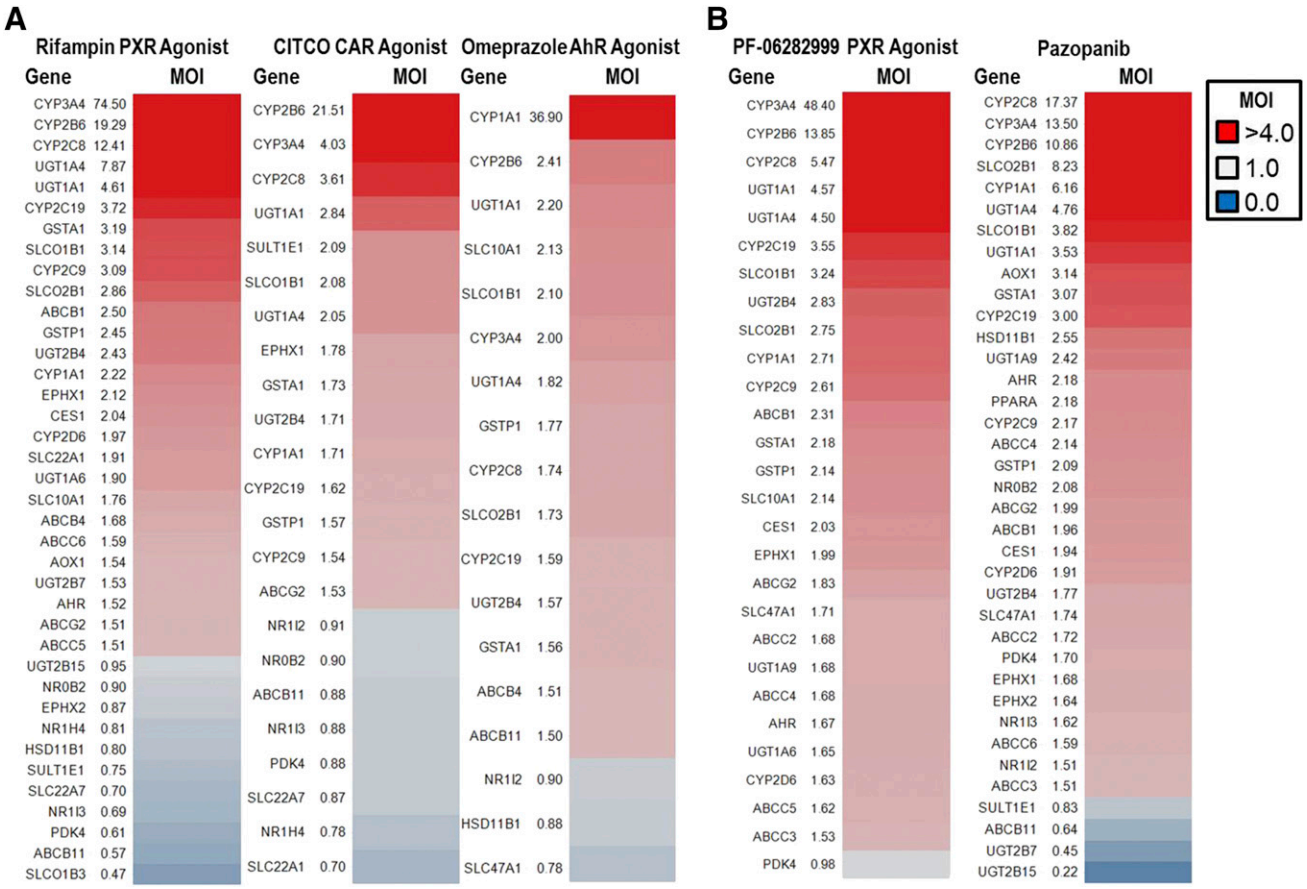

Fig. 3. MOI signatures with PXR, CAR, and AhR activation. *m*RNA expression was analyzed by qPCR with TaqMan array cards and was plotted versus the concentration dose response for selective activators rifampin (0.1–10 μM), CITCO (0.01–1 μM), omeprazole (0.03–3 μM) (A), and test compounds PF-06282999 (10–1000 μM) or pazopanib (0.1–10 μM) (B). Data are expressed as MOI at a single concentration normalized to 0.1% DMSO control. MOI was determined for each donor (n = 3) and averaged for a representative singular MOI per gene per treatment.

Under the current experimental conditions, the gene induction profile PF-06282999 most closely matched that of rifampin, although at lower magnitudes, given its weak PXR agonist activity (Fig. 3B). Thus, treatment of primary hepatocytes with PF-06282999 on average induced CYP3A4 48-fold, followed by CYP2B6 (14-fold) and CYP2C8 (5.5-fold), as well as UGT1A1, UGT1A4, and CYP2C19 between 3- and 5-fold. As expected, PF-06282999 induced the same genes as

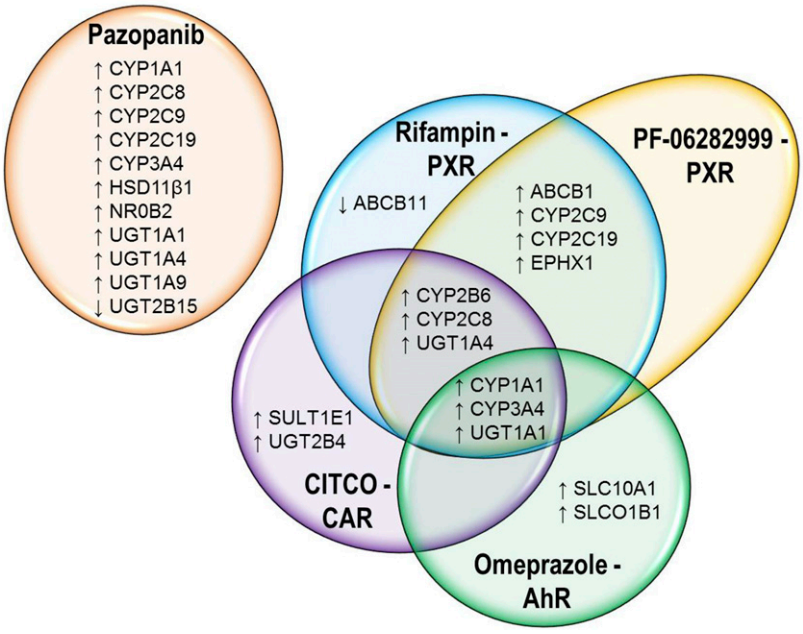

Fig. 4. Illustration of differentiating and overlapping gene expression signatures for PXR, CAR, and AhR. MOI of *m*RNA expression was analyzed by a two-way ANOVA, followed by a Dunnett's multiple comparison test, to compare overall mean differences between treatment groups. Significance was set at $P < 0.05$. Categories were determined by the following criteria: 1) fold change in *m*RNA expression $\geq$ 2-fold compared with respective 0.1% DMSO control; 2) fold change observed in two or more donors at one or more concentrations.

TABLE 2

In vitro *m*RNA induction parameters, EC_{50} and E_{max}, can differentiate commonly regulated genes

The EC_{50} and E_{max} values were determined for each gene regulated by PXR and CAR or PXR, CAR, and AhR for each donor. Dose-response curves were generated for *m*RNA expression (fold induction normalized to 0.1% DMSO) vs. the concentration-response for selective activators rifampin (0.1–10 μM), CITCO (0.01–1 μM) and omeprazole (0.03–3 μM), and individual fitting was carried out. E_{max} (relative fold induction of *m*RNA), EC_{50} (μM), S.E.

Gene		Rifampin			CITCO			Omeprazole		
		BNA	FOS	HH1089	BNA	FOS	HH1089	BNA	FOS	HH1089
CYP1A1	E_{max} ± S.E.	2.40 ± 0.39	3.08 ± 0.45	0.81 ± 0.10[a]	1.83 ± 0.13	1.66 ± 0.18a	2.37 ± 0.53	70.3 ± 9.10[a]	43.2 ± 7.50	36.9 ± 16.7
	EC_{50} ± S.E.	0.51 ± 0.55	0.75 ± 0.60	*NA*	0.01 ± 0.005	NA	0.28 ± 0.29	NA	2.13 ± 0.53	6.39 ± 4.15
CYP3A4	E_{max} ± S.E.	100 ± 7.54	78.1 ± 5.60	35.2 ± 2.88	5.31 ± 0.44	5.37 ± 0.46	3.75 ± 0.31	2.25 ± 0.37	2.64 ± 0.48	1.67 ± 0.10[a]
	EC_{50} ± S.E.	0.21 ± 0.08	0.13 ± 0.05	0.2 ± 0.08	0.18 ± 0.05	0.17 ± 0.06	0.07 ± 0.03	0.74 ± 0.62	0.82 ± 0.67	*NA*
UGT1A1	E_{max} ± S.E.	4.87 ± 0.34	5.05 ± 0.32	3.24 ± 0.28	2.83 ± 0.22	2.12 ± 0.11	3.31 ± 0.26	2.08 ± 0.16[a]	3.68 ± 1.20	2.56 ± 0.31
	EC_{50} ± S.E.	0.57 ± 0.19	0.26 ± 0.09	0.18 ± 0.11	0.08 ± 0.04	0.07 ± 0.02	0.04 ± 0.02	NA	3.12 ± 2.41	0.65 ± 0.37
CYP2B6	E_{max} ± S.E.	26.5 ± 2.33	19.8 ± 2.98	7.29 ± 0.84	33.3 ± 3.06	17.2 ± 0.68	13.1 ± 0.62			
	EC_{50} ± S.E.	0.42 ± 0.16	0.41 ± 0.27	0.33 ± 0.19	0.08 ± 0.03	0.03 ± 0.006	0.04 ± 0.008			
CYP2C8	E_{max} ± S.E.	4.47 ± 0.43	11.0 ± 2.00	13.7 ± 3.39	5.31 ± 0.39	2.13 ± 0.08	3.16 ± 0.17			
	EC_{50} ± S.E.	0.07 ± 0.06	0.15 ± 0.15	0.20 ± 0.24	0.04 ± 0.01	0.03 ± 0.01	0.02 ± 0.007			
UGT1A4	E_{max} ± S.E.	5.56 ± 0.26	10.3 ± 0.97	6.07 ± 0.61	2.01 ± 0.19	1.72 ± 0.10	2.57 ± 0.16			
	EC_{50} ± S.E.	0.67 ± 0.14	0.38 ± 0.17	0.25 ± 0.14	0.10 ± 0.06	0.12 ± 0.05	0.07 ± 0.03			

[a]NA, not applicable in the absence of E_{max}.
MOI is reported where E_{max} was not reached.

rifampin (Fig. 4), suggesting activation of the same gene regulation pathway and consistent with our previous study (Moscovitz et al., 2017). A significant downregulation of ABCB11 was not detected with PF-06282999, likely because of its weaker PXR activation. In contrast, the TKI pazopanib demonstrated a distinct gene expression signature by enhancing CYP2C8 by 17-fold, followed by CYP3A4 and CYP2B6 >10-fold, and CYP1A1 by 6-fold (Fig. 3B). Unlike the selective NR activators, pazopanib also induced the gene expression of HSD11β1, UGT1A9, and NR0B2 (>20-fold). Marked downregulation of UGT2B15 (78%) was observed with pazopanib treatment. Thus, pazopanib enhanced genes commonly regulated by PXR, CAR, and AhR (CYP1A1, CYP3A4, UGT1A1), PXR, and CAR (CYP2C8, UGT1A4), PXR (CYP2C9, CYP2C19), but also distinct genes such as HSD11β1, NR0B2, UGT1A9, with profound down-regulation of UGT2B15 (Fig. 4).

Minimal DME and Transporter Gene List to Enable Differentiation between PXR and CAR. Further analyses of the full dose response curves (where possible) for genes that were inducible via PXR and CAR or PXR, CAR, and AhR were performed to assess whether it could provide further differentiation. For these genes, concentration response curves were generated for *m*RNA expression (fold induction normalized to 0.1% DMSO) versus the concentrations for rifampin, CITCO, and omeprazole, and individual fitting was carried out on each hepatocyte donor using a three-parameter or four-parameter sigmoidal model. The in vitro parameters EC_{50} and E_{max} were calculated for each donor concentration response curve (Table 2). Where E_{max} could not be reached (BNA, omeprazole for CYP1A1 and UGT1A1; FOS, CITCO for CYP1A1; HH1089, rifampin for CYP1A1, omeprazole for CYP3A4), MOI is reported in the table.

CYP1A1, CYP3A4, and UGT1A1 were commonly regulated by PXR, CAR, and AhR, whereas PXR and CAR both induced CYP2B6, CYP2C8, and UGT1A4. Across all three donors, and in line with the MOI data, rifampin activation of PXR resulted in the highest E_{max} of CYP3A4 (35- to 100-fold) and lowest EC_{50} (0.13–0.21 μM). Similarly, CITCO treatment of cryopreserved human hepatocytes produced a higher CYP2B6 E_{max} with a lower EC_{50}, 13- to 33-fold and 0.03–0.08 μM, respectively, than rifampin treatment. Although the EC_{50} for omeprazole induction of CYP1A1 ranged from 2 to 6 μM across donors, the E_{max} (37- to 43-fold) was significantly higher than that of rifampin and CITCO treatment, which resulted in E_{max} values of between ~2- and 3-fold. For UGT1A1, the E_{max} was higher for rifampin; however, CITCO EC_{50} values were lowest but resulted in *m*RNA induction of only 2- to 3-fold. To apply the use of both EC_{50} and E_{max} values for mRNA expression versus the concentration response curves, genes that were commonly regulated by both PXR and CAR were plotted for rifampin-, CITCO-, and PF-06282999-treated cells for all three primary human hepatocyte donor lots (Fig. 5). For rifampin and PF-06282999, responsiveness of target genes across hepatocyte lots was as follows: CYP3A4 > CYP2B6 > CYP2C8 > UGT1A1 = UGT1A4 = CYP1A1. With CITCO treatment, the responsiveness of target genes differed: CYP2B6 > CYP3A4 = CYP2C8 = UGT1A1 > UGT1A4 > CYP1A1.

Discussion

Consistent with the literature, our present study demonstrated that treatment of human hepatocytes with rifampin,

CITCO, and omeprazole resulted in MOI of CYP3A4, CYP2B6, and CYP1A1 *m*RNA (Gonzalez et al., 1984; Sutter et al., 1994; Bertilsson et al., 1998; Lehmann et al., 1998; Maglich et al., 2002, 2003; Badolo et al., 2015). Rifampin-mediated PXR activation in human hepatocytes also resulted in the greatest number of differentially regulated genes, including ABCB1, CYP2C9, and CYP2C19, which was generally consistent with prior results (Gerbal-Chaloin et al., 2001; Synold et al., 2001; Raucy et al., 2002; Jigorel et al., 2006; Yajima et al., 2014). The differential induction of EPHX1 *m*RNA by rifampin in our study is consistent with the previous observations on the induction of this detoxification enzyme in mice after subchronic treatment with the rodent Pxr activator pregnenolone 16α-carbonitrile (Xie et al., 2000; Cui and Klaassen, 2016). Human liver microsomal EPHX1 hydrolyzes protein- and/or DNA-reactive epoxides (Seidegard and Ekstrom, 1997) that are obtained via P450-mediated oxidations on aromatic/heteroaromatic rings and/or olefinic substituents in drugs such as phenytoin and carbamazepine (Fretland and Omiecinski, 2000). Whether increased EPHX1 *m*RNA via PXR activation in human hepatocytes leads to a higher rate of detoxification of electrophilic epoxides generated via CYP3A/2C-mediated xenobiotic bioactivation remains to be assessed. ABCB11 *m*RNA repression with rifampin was the only robust downregulation noted in hepatocyte donors with prototypical inducer treatment and has been observed in a previous study (Jigorel et al., 2006); however, conflicting reports have also been published in human liver slices demonstrating no change (Marschall et al., 2005) or upregulation (Olinga et al., 2008) of ABCB11 *m*RNA.

Upregulation of SULT1E1 mRNA by the CAR activator CITCO in human hepatocytes is consistent with previous data indicating gender-specific Sult1e1 activation in female mouse liver in response to Car ligands diallyl sulfide (Sueyoshi et al., 2011) or 1,4-*bis*[2-(3,5-dichloropyridyloxy)]benzene (Baskin-Bey et al., 2006; Alnouti and Klaassen, 2008). Upregulation of SULT1E1 *m*RNA by CITCO in both female (HH1089) and male (BNA) human hepatocyte lots implies that gender-specific upregulation of SULT1E1 via CAR activation may be restricted to rodents specifically. Increases in *m*RNA of UGT2B4 noted with CITCO in our study have not been observed previously in animals or human reagents. Assessment of UGT2B4 regulation in human hepatocytes in regard to bile acid metabolism identified NRs (farnesoid X receptor and PPARα) commonly involved in endogenous cholesterol pathways (Barbier et al., 2003a,b). AhR activation by omeprazole was uniquely associated with increases in *m*RNA for SLC10A1, which is consistent with the work of Olinga et al. (2008), who identified SLC10A1 upregulation in human liver slices

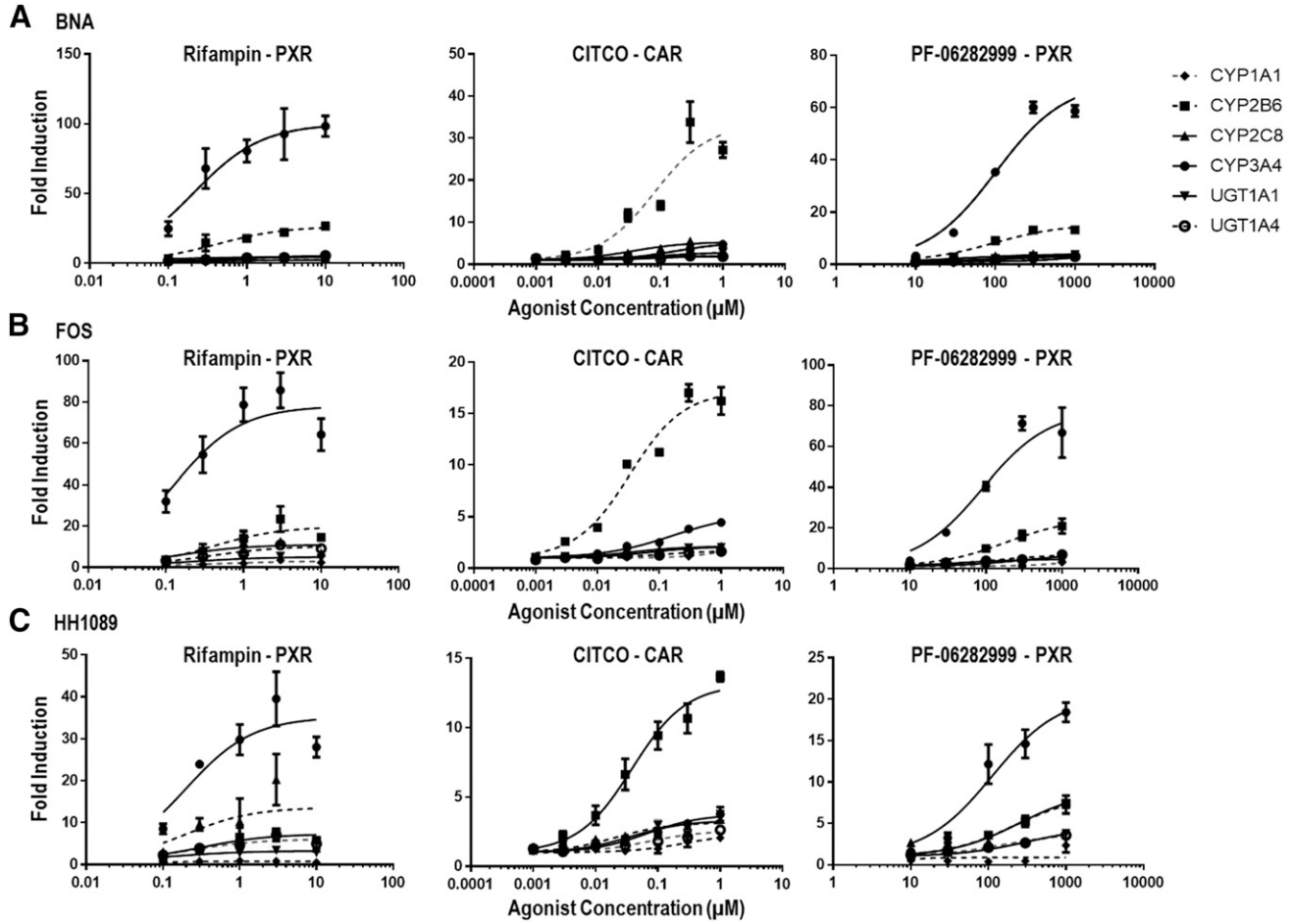

Fig. 5. In vitro *m*RNA induction dose-response curves for differentiating PXR and CAR agonists. *m*RNA expression was analyzed by qPCR with TaqMan array cards and was plotted versus the concentration dose response for rifampin (0.1–10 μM), CITCO (0.01–1 μM), or PF-06282999 (10–1000 μM) for donors BNA (A), FOS (B), and HH1089 (C). Individual fitting was carried out on each hepatocyte donor (A–C) and was fit to either a four-parameter sigmoidal model or a three-parameter sigmoidal model.

treated with the AhR agonist β-napthoflavone (Olinga et al., 2008). The upregulation of SLCO1B1 by omeprazole, also noted in our work, appears to be a novel finding.

Previous reports using *m*RNA and protein assessment in primary human hepatocytes, HepG2 cells, and reporter assays revealed that CYP2B6, CYP3A4, and UGT1A1 gene expression was coregulated by PXR and CAR (Honkakoski et al., 1998; Goodwin et al., 2001; Sugatani et al., 2005; Sinz et al., 2006; Sinz, 2015). In addition, the induction of UGT1A1 gene expression in human hepatoma HepG2 cells has been noted with AhR activation (Yueh et al., 2003). Studies have also identified the response elements in UGT1A1 corresponding to each NR (Sugatani et al., 2001; Xie et al., 2003; Yueh et al., 2003), as well as PXR response elements in CYP3A4, CYP2B6, and UGT1A1 in primary human hepatocytes (Hariparsad et al., 2009). The six DME targets (CYP1A1/2B6/2C8/3A4, UGT1A1/1A4) that were induced (albeit at varying magnitudes) by PXR and CAR or PXR, CAR, and AhR in our work are responsible for the metabolism of >70% of marketed drugs (Williams et al., 2004; Guengerich, 2008). Activator concentration response relationships (E_{max} and EC_{50}) for *m*RNA expression were determined, which provided relevance with respect to the concentrations needed to elicit, and the maximal effect possible for activation of each gene by PXR, CAR, and AhR. For example, rifampin-treated human hepatocytes resulted in a dramatic lot dependent E_{max} of 35- to 100-fold and EC_{50} of 0.13–0.21 μM for CYP3A4 *m*RNA expression. Although the EC_{50} for CYP3A4 *m*RNA increase with CITCO treatment was comparable to that of rifampin (0.07–0.18 μM), the E_{max} ranged from only 3.8- to 5.4-fold. This approach highlights the importance of assessing EC_{50} in conjunction with E_{max} for an accurate depiction of NR target gene sensitivity and possibly for quantitative prediction of DDIs.

The myeloperoxidase inactivator PF-06282999 performed identically to rifampin, inducing a comparable gene expression profile, albeit to a lesser extent (consistent with its weak PXR agonist activity). The profile consisted of genes identified as PXR-specific; PXR- and CAR-overlapping; and PXR, CAR, and AhR overlapping. Importantly, the genes suggesting CAR or AhR activation alone were not induced by PF-06282999. This compound also differentiated itself from the selective CAR agonist CITCO in its concentration response curves for overlapping PXR and CAR target genes. In these analyses, the relative rank-ordered sensitivity of ADME genes was identical for rifampin and PF-06282999, but not CITCO, in all three donor lots.

Clinical DDIs arising from induction of major P450 enzymes by NR activators are plentiful (Pelkonen et al., 2008); however, DDIs arising from upregulation of non-P450 enzymes are scarce with drugs (or drug candidates). Wenning et al. (2009) demonstrated a ~40% reduction in plasma area under the curve (AUC) and C_{max} of the selective UGT1A1 substrate raltegravir in humans pretreated with rifampin (600 mg daily for 14 days) (Wenning et al., 2009). In comparison, the same dose of rifampin (dosed daily for 5 days) reduces the AUC and C_{max} of the CYP3A4 probe substrate midazolam by 96% and 94%, respectively (Backman et al., 1996). The clinical interaction between rifampin and selective substrates of UGT1A1 and/or CYP3A4 supports our in vitro observations in which human hepatocytes treated with rifampin (10 μM) for 48 hours resulted in the induction of both CYP3A4 and UGT1A1 *m*RNA by 35- to 100- and 3- to 5-fold, respectively. The in vivo DDI study with raltegravir also confirms previous literature (Marschall et al., 2005; Sugatani et al., 2005; Hariparsad et al., 2009) that has revealed increased UGT1A1 *m*RNA and enzyme activity in response to PXR activators. Cumulatively, the combined data also suggest that maximal DDIs with a PXR activator will occur at the level of CYP3A4 followed by enzymes activated at lesser magnitudes. Contextualizing the in vitro EC_{50} and E_{max} values for rifampin-induced UGT1A1 *m*RNA and enzyme activity in relation to its human unbound plasma concentrations can shed additional light on the DDI with raltegravir.

Finally, pazopanib was included in this analysis because of a previous report suggestive of CYP3A4 induction in vitro (https://www.accessdata.fda.gov/drugsatfda_docs/nda/2009/022465s000_ClinPharmR.pdf) (NDA-022465, 2009). To our surprise, treatment of human hepatocytes with pazopanib resulted in a profile distinct from PXR, CAR, or AhR activators. Pazopanib induced P450 (CYP2C8/2C9/2C19/3A4) and UGT (UGT1A1/1A4/1A9) isoforms while significantly downregulating UGT2B15. Non-DME target genes such as HSD11β1 and NR0B2, typical target genes of alternate NR pathways, were also susceptible toward induction by pazopanib. These data suggest that CYP3A4 induction by pazopanib is not mediated through PXR activation. Consistent with this hypothesis, recent transactivation data from our laboratory have revealed that pazopanib is not a PXR activator (unpublished observations). Studies are under way to identify the transcriptional regulator(s) for pazopanib and structurally diverse TKIs. Downregulation of UGT2B15 *m*RNA will require correlation with corresponding decreases in UGT2B15 catalytic activity in relation to potential DDIs with drugs metabolized by UGT2B15. It is important to note that the package insert for pazopanib does not highlight DDIs arising from CYP3A4 induction as a liability. Rather, reports on clinical DDIs arising from inhibition of CYP3A4 (Keisner and Shah, 2011) and CYP2C8 by pazopanib have appeared in the literature (Tan et al., 2010; Hamberg et al., 2015) and reflect a dominance of CYP3A4 inhibition over CYP3A4 induction as a causative factor for a DDI.

Current mathematical models (Fahmi et al., 2008a,b) used to project the magnitude of clinical DDIs arising from in vitro induction of CYP3A4 *m*RNA and catalytic activity for selective PXR activators can be potentially extended to include other phase I (e.g., P450) and phase II (e.g., UGT) enzymes (Hariparsad et al., 2017); however, this method may not be applicable for compounds that induce CYP3A4 through selective CAR activation or via an unknown pathway/mechanism (e.g., pazopanib). This would also hold true for downregulation events, for which there is no known correlation with the magnitude of CYP3A4 upregulation. Therefore, identifying the mechanism by which compounds upregulate or downregulate DMEs and transporters will be a crucial prerequisite for predicting DDIs. Studies are currently under way to determine changes in UGT1A1/2B15 activities that could potentially accompany upregulation and downregulation of UGT mRNA by rifampin and pazopanib, respectively, in human hepatocytes.

In conclusion, this is the first detailed report that enables a holistic and mechanism-based assessment of DDI risk as a result of transcriptional regulation of DME and transporter genes beyond the conventional P450 (CYP3A4/2B6/1A2) enzymes and represents the first step toward addressing the

concerns outlined by the regulatory agencies. Our present method can be conveniently adapted to the current standard practice used in the pharmaceutical industry since the protocol used in our studies was an established work flow involving the use of human hepatocytes to characterize P450 enzyme inducers.

Acknowledgments

We thank Dr. Larry Tremaine and Dr. Dennis Scott for critical discussions and feedback pertaining to this work.

Authorship Contributions

Participated in research design: Weng, Kalgutkar, Moscovitz, Goosen.

Conducted experiments: Moscovitz, Johnson.

Contributed new reagents or analytic tools: Nulick, Lin.

Performed data analysis: Moscovitz, Johnson, Weng, Kalgutkar.

Wrote or contributed to the writing of the manuscript: Moscovitz, Kalgutkar, Weng.

References

Aleksunes LM and Klaassen CD (2012) Coordinated regulation of hepatic phase I and II drug-metabolizing genes and transporters using AhR-, CAR-, PXR-, PPARα-, and Nrf2-null mice. *Drug Metab Dispos* **40**:1366–1379.

Alnouti Y and Klaassen CD (2008) Regulation of sulfotransferase enzymes by prototypical microsomal enzyme inducers in mice. *J Pharmacol Exp Ther* **324**: 612–621.

Backman JT, Olkkola KT, and Neuvonen PJ (1996) Rifampin drastically reduces plasma concentrations and effects of oral midazolam. *Clin Pharmacol Ther* **59**: 7–13.

Badolo L, Jensen B, Säll C, Norinder U, Kallunki P, and Montanari D (2015) Evaluation of 309 molecules as inducers of CYP3A4, CYP2B6, CYP1A2, OATP1B1, OCT1, MDR1, MRP2, MRP3 and BCRP in cryopreserved human hepatocytes in sandwich culture. *Xenobiotica* **45**:177–187.

Barbier O, Duran-Sandoval D, Pineda-Torra I, Kosykh V, Fruchart JC, and Staels B (2003a) Peroxisome proliferator-activated receptor alpha induces hepatic expression of the human bile acid glucuronidating UDP-glucuronosyltransferase 2B4 enzyme. *J Biol Chem* **278**:32852–32860.

Barbier O, Torra IP, Sirvent A, Claudel T, Blanquart C, Duran-Sandoval D, Kuipers F, Kosykh V, Fruchart JC, and Staels B (2003b) FXR induces the UGT2B4 enzyme in hepatocytes: a potential mechanism of negative feedback control of FXR activity. *Gastroenterology* **124**:1926–1940.

Baskin-Bey ES, Huang W, Ishimura N, Isomoto H, Bronk SF, Braley K, Craig RW, Moore DD, and Gores GJ (2006) Constitutive androstane receptor (CAR) ligand, TCPOBOP, attenuates Fas-induced murine liver injury by altering Bcl-2 proteins. *Hepatology* **44**:252–262.

Bertilsson G, Heidrich J, Svensson K, Asman M, Jendeberg L, Sydow-Bäckman M, Ohlsson R, Postlind H, Blomquist P, and Berkenstam A (1998) Identification of a human nuclear receptor defines a new signaling pathway for CYP3A induction. *Proc Natl Acad Sci USA* **95**:12208–12213.

Chu V, Einolf HJ, Evers R, Kumar G, Moore D, Ripp S, Silva J, Sinha V, Sinz M, and Skerjanec A (2009) In vitro and in vivo induction of cytochrome p450: a survey of the current practices and recommendations: a pharmaceutical research and manufacturers of america perspective. *Drug Metab Dispos* **37**:1339–1354.

Cui JY and Klaassen CD (2016) RNA-Seq reveals common and unique PXR- and CAR-target gene signatures in the mouse liver transcriptome. *Biochim Biophys Acta* **1859**:1198–1217.

Dong JQ, Gosset JR, Fahmi OA, Lin Z, Chabot JR, Terra SG, Le V, Chidsey K, Nouri P, Kim A, et al. (2017) Examination of the human cytochrome P4503A4 induction potential of PF-06282999, an irreversible myeloperoxidase inactivator: integration of preclinical, in silico, and biomarker methodologies in the prediction of the clinical outcome. *Drug Metab Dispos* **45**:501–511.

Dong JQ, Varma MV, Wolford A, Ryder T, Di L, Feng B, Terra SG, Sagawa K, and Kalgutkar AS (2016) Pharmacokinetics and disposition of the thiouracil derivative PF-06282999, an orally bioavailable, irreversible inactivator of myeloperoxidase enzyme, across animals and humans. *Drug Metab Dispos* **44**:209–219.

European Medicines Agency (EMA) (2012) Guideline on the Investigation of Drug Interactions, Committee for Human Medicinal Products. London.

Fahmi OA, Boldt S, Kish M, Obach RS, and Tremaine LM (2008a) Prediction of drug-drug interactions from in vitro induction data: application of the relative induction score approach using cryopreserved human hepatocytes. *Drug Metab Dispos* **36**: 1971–1974.

Fahmi OA, Maurer TS, Kish M, Cardenas E, Boldt S, and Nettleton D (2008b) A combined model for predicting CYP3A4 clinical net drug-drug interaction based on CYP3A4 inhibition, inactivation, and induction determined in vitro. *Drug Metab Dispos* **36**:1698–1708.

Fahmi OA and Ripp SL (2010) Evaluation of models for predicting drug-drug interactions due to induction. *Expert Opin Drug Metab Toxicol* **6**:1399–1416.

Fretland AJ and Omiecinski CJ (2000) Epoxide hydrolases: biochemistry and molecular biology. *Chem Biol Interact* **129**:41–59.

Gerbal-Chaloin S, Pascussi JM, Pichard-Garcia L, Daujat M, Waechter F, Fabre JM, Carrère N, and Maurel P (2001) Induction of CYP2C genes in human hepatocytes in primary culture. *Drug Metab Dispos* **29**:242–251.

Giacomini KM, Huang SM, Tweedie DJ, Benet LZ, Brouwer KL, Chu X, Dahlin A, Evers R, Fischer V, Hillgren KM, et al.; International Transporter Consortium (2010) Membrane transporters in drug development. *Nat Rev Drug Discov* **9**:215–236.

Gonzalez FJ, Tukey RH, and Nebert DW (1984) Structural gene products of the Ah locus. Transcriptional regulation of cytochrome P1-450 and P3-450 mRNA levels by 3-methylcholanthrene. *Mol Pharmacol* **26**:117–121.

Goodwin B, Hodgson E, D'Costa DJ, Robertson GR, and Liddle C (2002a) Transcriptional regulation of the human CYP3A4 gene by the constitutive androstane receptor. *Mol Pharmacol* **62**:359–365.

Goodwin B, Hodgson E, and Liddle C (1999) The orphan human pregnane X receptor mediates the transcriptional activation of CYP3A4 by rifampicin through a distal enhancer module. *Mol Pharmacol* **56**:1329–1339.

Goodwin B, Moore LB, Stoltz CM, McKee DD, and Kliewer SA (2001) Regulation of the human CYP2B6 gene by the nuclear pregnane X receptor. *Mol Pharmacol* **60**:427–431.

Goodwin B, Redinbo MR, and Kliewer SA (2002b) Regulation of cyp3a gene transcription by the pregnane x receptor. *Annu Rev Pharmacol Toxicol* **42**:1–23.

Guengerich FP (2008) Cytochrome p450 and chemical toxicology. *Chem Res Toxicol* **21**: 70–83.

Hamberg P, Mathijssen RH, de Bruijn P, Leonowens C, van der Biessen D, Eskens FA, Sleijfer S, Verweij J, and de Jonge MJ (2015) Impact of pazopanib on docetaxel exposure: results of a phase I combination study with two different docetaxel schedules. *Cancer Chemother Pharmacol* **75**:365–371.

Hariparsad N, Chu X, Yabut J, Labhart P, Hartley DP, Dai X, and Evers R (2009) Identification of pregnane-X receptor target genes and coactivator and corepressor binding to promoter elements in human hepatocytes. *Nucleic Acids Res* **37**:1160–1173.

Hariparsad N, Ramsden D, Palamanda J, Dekeyser JG, Fahmi OA, Kenny JR, Einolf H, Mohutsky M, Pardon M, Siu YA, et al. (2017) Considerations from the IQ induction working group in response to drug-drug interaction guidance from regulatory agencies: focus on downregulation, CYP2C induction, and CYP2B6 positive control. *Drug Metab Dispos* **45**:1049–1059.

Honkakoski P, Zelko I, Sueyoshi T, and Negishi M (1998) The nuclear orphan receptor CAR-retinoid X receptor heterodimer activates the phenobarbital-responsive enhancer module of the CYP2B gene. *Mol Cell Biol* **18**:5652–5658.

Jigorel E, Le Vee M, Boursier-Neyret C, Parmentier Y, and Fardel O (2006) Differential regulation of sinusoidal and canalicular hepatic drug transporter expression by xenobiotics activating drug-sensing receptors in primary human hepatocytes. *Drug Metab Dispos* **34**:1756–1763.

Kandel BA, Thomas M, Winter S, Damm G, Seehofer D, Burk O, Schwab M, and Zanger UM (2016) Genomewide comparison of the inducible transcriptomes of nuclear receptors CAR, PXR and PPARα in primary human hepatocytes. *Biochim Biophys Acta* **1859**:1218–1227.

Keisner SV and Shah SR (2011) Pazopanib: the newest tyrosine kinase inhibitor for the treatment of advanced or metastatic renal cell carcinoma. *Drugs* **71**:443–454.

Lehmann JM, McKee DD, Watson MA, Willson TM, Moore JT, and Kliewer SA (1998) The human orphan nuclear receptor PXR is activated by compounds that regulate CYP3A4 gene expression and cause drug interactions. *J Clin Invest* **102**: 1016–1023.

Liu XJ, Lu H, Sun JX, Wang SR, Mo YS, Yang XS, and Shi BK (2016) Metabolic behavior prediction of pazopanib by cytochrome P450 (CYP) 3A4 by molecular docking. *Eur J Drug Metab Pharmacokinet* **41**:465–468.

Maglich JM, Parks DJ, Moore LB, Collins JL, Goodwin B, Billin AN, Stoltz CA, Kliewer SA, Lambert MH, Willson TM, et al. (2003) Identification of a novel human constitutive androstane receptor (CAR) agonist and its use in the identification of CAR target genes. *J Biol Chem* **278**:17277–17283.

Maglich JM, Stoltz CM, Goodwin B, Hawkins-Brown D, Moore JT, and Kliewer SA (2002) Nuclear pregnane x receptor and constitutive androstane receptor regulate overlapping but distinct sets of genes involved in xenobiotic detoxification. *Mol Pharmacol* **62**:638–646.

Marschall HU, Wagner M, Zollner G, Fickert P, Diczfalusy U, Gumhold J, Silbert D, Fuchsbichler A, Benthin L, Grundström R, et al. (2005) Complementary stimulation of hepatobiliary transport and detoxification systems by rifampicin and ursodeoxycholic acid in humans. *Gastroenterology* **129**:476–485.

Moscovitz JE, Lin Z, Johnson N, Tu M, Goosen TC, Weng Y, and Kalgutkar AS (2017) Induction of human cytochrome P450 3A4 by the irreversible myeloperoxidase inactivator PF-06282999 is mediated by the pregnane X receptor. *Xenobiotica* 1–9 DOI: 10.1124/pr.55.3.4.

New Drug Application (NDA)-022465 (2009) Clinical Pharmacology and Biopharmaceutics Reviews, Center for Drug Evaluation and Research, Food and Drug Administration, Bethesda, MD.

Olinga P, Elferink MG, Draaisma AL, Merema MT, Castell JV, Pérez G, and Groothuis GM (2008) Coordinated induction of drug transporters and phase I and II metabolism in human liver slices. *Eur J Pharm Sci* **33**:380–389.

Pelkonen O, Turpeinen M, Hakkola J, Honkakoski P, Hukkanen J, and Raunio H (2008) Inhibition and induction of human cytochrome P450 enzymes: current status. *Arch Toxicol* **82**:667–715.

Raucy JL, Mueller L, Duan K, Allen SW, Strom S, and Lasker JM (2002) Expression and induction of CYP2C P450 enzymes in primary cultures of human hepatocytes. *J Pharmacol Exp Ther* **302**:475–482.

Ruggeri RB, Buckbinder L, Bagley SW, Carpino PA, Conn EL, Dowling MS, Fernando DP, Jiao W, Kung DW, Orr ST, et al. (2015) Discovery of 2-(6-(5-Chloro-2-methoxyphenyl)-4-oxo-2-thioxo-3,4-dihydropyrimidin-1(2H)-yl)acetamide (PF-06282999): a highly selective mechanism-based myeloperoxidase inhibitor for the treatment of cardiovascular diseases. *J Med Chem* **58**:8513–8528.

Seidegård J and Ekström G (1997) The role of human glutathione transferases and epoxide hydrolases in the metabolism of xenobiotics. *Environ Health Perspect* **105** (Suppl 4):791–799.

Sinz M (2015) Avoiding PXR and CAR activation and CYP3A4 enzyme induction. *Top Med Chem* **9**:159–190.

Sinz M, Kim S, Zhu Z, Chen T, Anthony M, Dickinson K, and Rodrigues AD (2006) Evaluation of 170 xenobiotics as transactivators of human pregnane X receptor

(hPXR) and correlation to known CYP3A4 drug interactions. *Curr Drug Metab* **7**: 375–388.
Sueyoshi T, Green WD, Vinal K, Woodrum TS, Moore R, and Negishi M (2011) Garlic extract diallyl sulfide (DAS) activates nuclear receptor CAR to induce the Sult1e1 gene in mouse liver. *PLoS One* **6**:e21229.
Sugatani J, Kojima H, Ueda A, Kakizaki S, Yoshinari K, Gong QH, Owens IS, Negishi M, and Sueyoshi T (2001) The phenobarbital response enhancer module in the human bilirubin UDP-glucuronosyltransferase UGT1A1 gene and regulation by the nuclear receptor CAR. *Hepatology* **33**:1232–1238.
Sugatani J, Sueyoshi T, Negishi M, and Miwa M (2005) Regulation of the human UGT1A1 gene by nuclear receptors constitutive active/androstane receptor, pregnane X receptor, and glucocorticoid receptor. *Methods Enzymol* **400**:92–104.
Sutter TR, Tang YM, Hayes CL, Wo YY, Jabs EW, Li X, Yin H, Cody CW, and Greenlee WF (1994) Complete cDNA sequence of a human dioxin-inducible mRNA identifies a new gene subfamily of cytochrome P450 that maps to chromosome 2. *J Biol Chem* **269**:13092–13099.
Synold TW, Dussault I, and Forman BM (2001) The orphan nuclear receptor SXR coordinately regulates drug metabolism and efflux. *Nat Med* **7**:584–590.
Tan AR, Dowlati A, Jones SF, Infante JR, Nishioka J, Fang L, Hodge JP, Gainer SD, Arumugham T, Suttle AB, et al. (2010) Phase I study of pazopanib in combination with weekly paclitaxel in patients with advanced solid tumors. *Oncologist* **15**: 1253–1261.
Wang YM, Ong SS, Chai SC, and Chen T (2012) Role of CAR and PXR in xenobiotic sensing and metabolism. *Expert Opin Drug Metab Toxicol* **8**:803–817.
Wenning LA, Hanley WD, Brainard DM, Petry AS, Ghosh K, Jin B, Mangin E, Marbury TC, Berg JK, Chodakewitz JA, et al. (2009) Effect of rifampin, a potent inducer of drug-metabolizing enzymes, on the pharmacokinetics of raltegravir. *Antimicrob Agents Chemother* **53**:2852–2856.
Wienkers LC and Heath TG (2005) Predicting in vivo drug interactions from in vitro drug discovery data. *Nat Rev Drug Discov* **4**:825–833.
Williams JA, Hyland R, Jones BC, Smith DA, Hurst S, Goosen TC, Peterkin V, Koup JR, and Ball SE (2004) Drug-drug interactions for UDP-glucuronosyltransferase substrates: a pharmacokinetic explanation for typically observed low exposure (AUCi/AUC) ratios. *Drug Metab Dispos* **32**:1201–1208.
Willson TM and Kliewer SA (2002) PXR, CAR and drug metabolism. *Nat Rev Drug Discov* **1**:259–266.
Xie W, Barwick JL, Downes M, Blumberg B, Simon CM, Nelson MC, Neuschwander-Tetri BA, Brunt EM, Guzelian PS, and Evans RM (2000) Humanized xenobiotic response in mice expressing nuclear receptor SXR. *Nature* **406**:435–439.
Xie W, Yeuh MF, Radominska-Pandya A, Saini SP, Negishi Y, Bottroff BS, Cabrera GY, Tukey RH, and Evans RM (2003) Control of steroid, heme, and carcinogen metabolism by nuclear pregnane X receptor and constitutive androstane receptor. *Proc Natl Acad Sci USA* **100**:4150–4155.
Xu C, Li CY, and Kong AN (2005) Induction of phase I, II and III drug metabolism/transport by xenobiotics. *Arch Pharm Res* **28**:249–268.
Yajima K, Uno Y, Murayama N, Uehara S, Shimizu M, Nakamura C, Iwasaki K, Utoh M, and Yamazaki H (2014) Evaluation of 23 lots of commercially available cryopreserved hepatocytes for induction assays of human cytochromes P450. *Drug Metab Dispos* **42**:867–871.
Yueh MF, Huang YH, Hiller A, Chen S, Nguyen N, and Tukey RH (2003) Involvement of the xenobiotic response element (XRE) in Ah receptor-mediated induction of human UDP-glucuronosyltransferase 1A1. *J Biol Chem* **278**:15001–15006.

Address correspondence to: Jamie Moscovitz, Medicine Design, Pfizer Worldwide Research and Development, 610 Main Street, Cambridge, MA 02139. E-mail: jamie.moscovitz@pfizer.com; or Yan Weng, BioMedicine Design, Pfizer Worldwide Research and Development, 610 Main Street, Cambridge, MA 02139. E-mail: yan.weng2@pfizer.com